nature climate change

SUPPLEMENTARY INFORMATION
https://doi.org/10.1038/s41558-019-0529-2

In the format provided by the authors and unedited.

Global loss of climate connectivity in tropical forests

Rebecca A. Senior [1,3]*, Jane K. Hill [2] and David P. Edwards [1]

[1]Department of Animal and Plant Sciences, Alfred Denny Building, University of Sheffield, Sheffield, UK. [2]Department of Biology, University of York, York, UK. [3]Present address: Woodrow Wilson School of Public and International Affairs, Princeton University, Princeton, NJ, USA.
*e-mail: rebecca.a.senior@gmail.com

Global loss of climate connectivity in tropical forests

Supplementary Information

Rebecca A. Senior[1]*, Jane K. Hill[2] and David P. Edwards[1]

[1]Department of Animal and Plant Sciences, Alfred Denny Building, University of Sheffield, Western Bank, Sheffield, S10 2TN, UK

[2]Department of Biology, University of York, Wentworth Way, York, YO10 5DD, UK

***Corresponding author:** rebecca.a.senior@gmail.com, +44(0)114 2220123 (R.A. Senior)

ORCID iDs: orcid.org/0000-0002-8208-736X (R.A. Senior); orcid.org/0000-0003-1871-7715 (J.K. Hill)

Contents

1 Supplementary Methods 1: Varying patch parameters

1.1 Methods

Following McGuire et al. (2016) we excluded forest patches less than 10 km^2. This was based on the assumption that excessively small patches are incapable of sustaining populations for long enough to enable range shifts through differential fitness at the leading and trailing edge of a species' range. However, the critical patch size to enable such demographic processes to occur will depend on the species in question, and indeed some species may shift their ranges via within-generation movement of migrating individuals. We tested the influence of minimum patch size by repeating the analyses for patch sizes of 1, 5, 10, 25 and 100 km^2. Note that a minimum size of 1 km^2 corresponds to no exclusions, since this is the resolution of the layers used. To speed up iteration over the different parameters we used a subset of the main data, which excluded land masses less than 10 km^2 and those with a temperature range less than the predicted temperature change under climate warming, since range shifts are unlikely to be sufficient responses to climate change in these land masses.

1.2 Results and Discussion

Current climate connectivity was captured by median climate connectivity in 2012, and the proportion of forested area that failed to achieve successful climate connectivity (≥ 0) in 2012. Median climate connectivity differed by realm for all patch sizes assessed ($p < 0.001$; Supplementary Figure 1a), and was below zero in all cases except where minimum patch size was 1 km^2. For species capable of surviving and reproducing in patch sizes of 1 km^2 or less, current forest cover is therefore sufficiently well-connected along climate gradients that these species should, on average, be able to shift their range within existing forest cover to avoid climate warming. For species requiring a larger critical patch size, tropical forest cover in all biogeographic realms was, on average, insufficient to facilitate such range shifts. For all patch sizes, median climate connectivity was generally lowest in the Neotropics, followed by the Afrotropics, Indomalaya, Australasia and Oceania (precise ranking depended on the minimum patch size applied; Supplementary Figure 1a).

The percentage of forest area with unsuccessful climate connectivity (< 0) in the year 2012 varied by biogeographic realm for all minimum patch sizes ($p < 0.001$). Precise ranking varied by minimum patch size (Supplementary Figure 1b), but generally the Afrotropics and Indomalaya had the highest proportion of forest failing to connect to future climate analogues, while the Neotropics and Australasia had the lowest. We suggest that low average values of climate connectivity in the Neotropics are somewhat compensated for by the large size of forest patches that do achieve successful climate connectivity. Although the proportion of successfully connected tropical forest was generally more than half of total forest area, a substantial portion of forest failed to achieve climate connectivity and the situation was worse for a larger minimum patch size and when including all land masses in the tropics (main text).

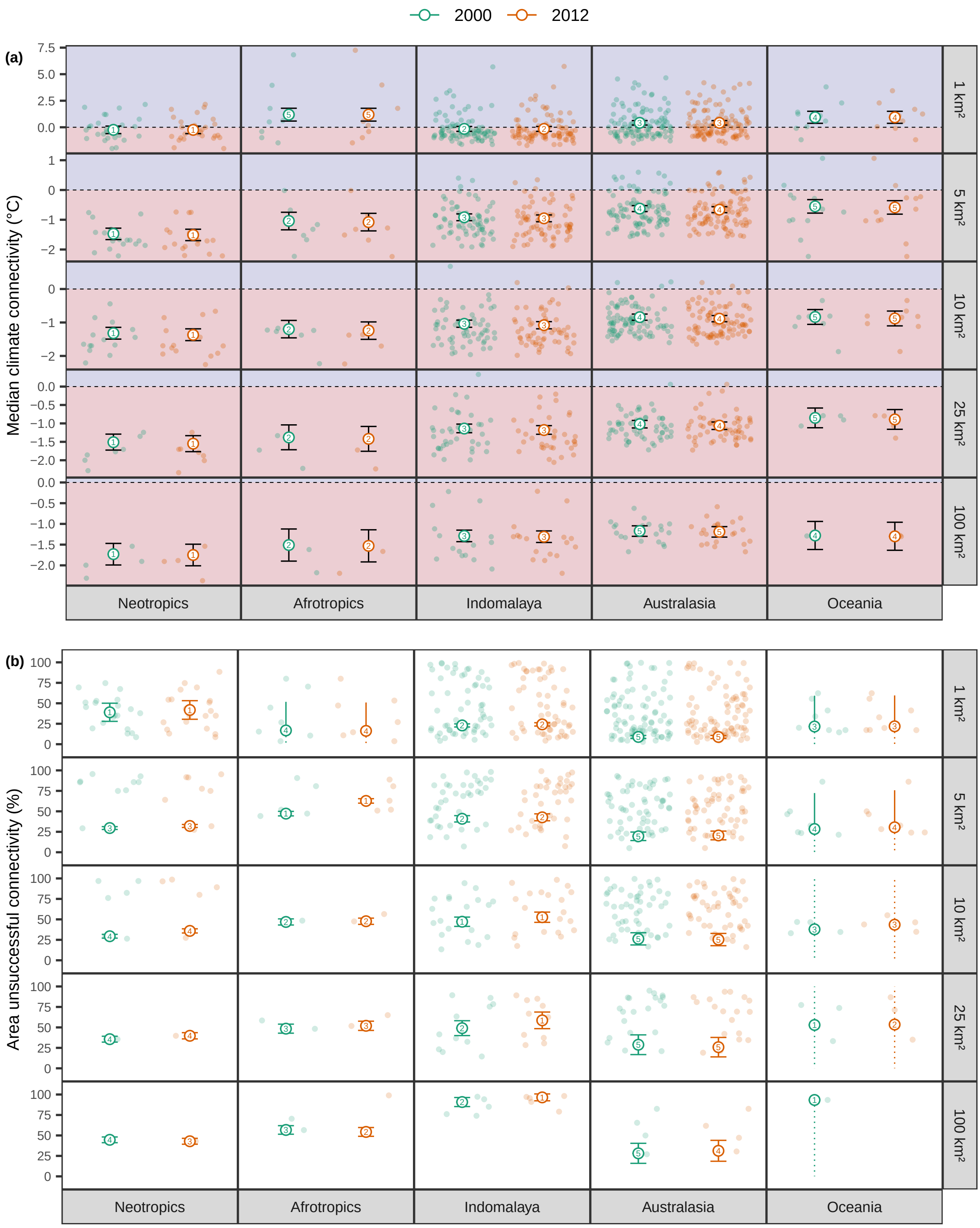

Supplementary Figure 1: Climate connectivity in the year 2000 (green) and 2012 (orange), for different values of minimum patch size (rows). Panel (a) shows results for median climate connectivity, with the dashed line indicating zero climate connectivity, at and above which successful climate connectivity is achieved. Panel (b) shows results for the proportion of total forested area that fails to achieve successful climate connectivity. Hollow circles are model-predicted values with 95% confidence intervals. The small number in the centre indicates rank: 1 corresponds to the realm and dataset with the worst climate connectivity, through to 5 for the best. Raw data are plotted in the background as semi-transparent, filled points. Confidence intervals in panel (b) are plotted with dotted lines where they extend beyond 0 or 100%.

From 2000 to 2012 we found that median climate connectivity did not change regardless of the minimum patch size applied ($p > 0.05$; Supplementary Figure 1a). The change in proportion of unsuccessfully connected forest was, however, more complicated. For extremes of minimum patch size – either 1 km^2 of 100 km^2 – there was no effect of year ($p > 0.05$; Supplementary Figure 1b). In the former case, it may be that any effect of year is masked by the greater amount of noise associated with an abundance of 1 km^2 patches. In the latter case it is likely that so few 100 km^2 patches were present at all that statistical power is lost, as well as the fact that patches of this size are likely to be more robust to relatively small changes in forest cover. For all other patch sizes, the proportion of successfully connected forest decreased from 2000 to 2012 ($p < 0.01$; Supplementary Figure 1b).

Loss of climate connectivity was strongly driven by loss of tree cover, regardless of minimum patch size ($p < 0.001$; Supplementary Figure 2). The proportion of forest area losing connectivity differed by realm for all minimum patch sizes ($p < 0.001$; Supplementary Figure 2), and was generally highest in Indomalaya, the Neotropics and the Afrotropics. In most cases climate connectivity was lost at an accelerating rate as the area of forest loss increased. For some patch sizes there was a hump-shaped relationship with tree cover loss, which is likely an artefact of there being fewer datapoints at high values of tree cover loss.

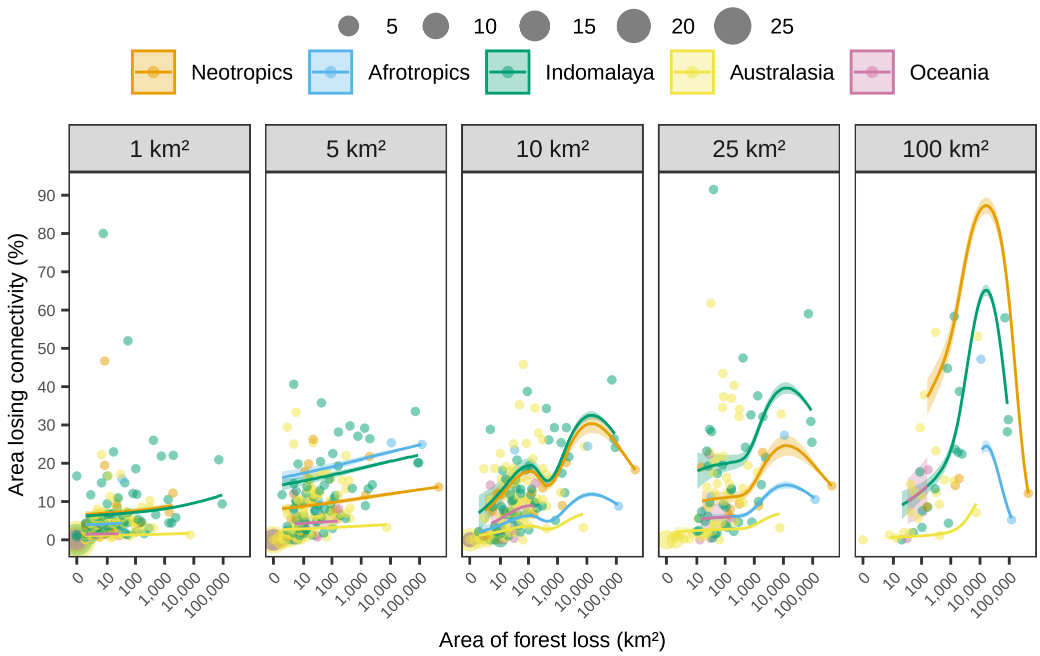

Supplementary Figure 2: The proportion of total forested area in each land mass that lost climate connectivity between 2000 and 2012, with increasing area of forest loss and across different biogeographic realms (orange = Neotropics, blue = Afrotropics, green = Indomalaya, yellow = Australasia and pink = Oceania). Points correspond to raw data, with point size indicating the number of observations at that value. Fitted lines derive from model predictions with 95% confidence intervals.

2 Supplementary Methods 2: Accounting for patch elevation

2.1 Methods

Forest patches at very high elevation will tend to have poor connectivity to future climate analogues because there is nowhere colder (i.e. higher) to connect to. To test the influence of elevation we repeated our analyses of current climate connectivity separately for patches at low and high elevation. Low elevation patches were defined as those with a median elevation less than or equal to the 75th percentile of elevation for the land mass in which it was located. High elevation patches had a median elevation exceeding this threshold. Subsequent analyses were otherwise analogous to those in the main text.

2.2 Results and Discussion

Both high and low elevation patches had median climate connectivity below zero, thus failing to achieve successful connectivity to future climate analogues. The difference between realms was only apparent for high elevation patches ($F = 2.72$, $p < 0.05$; Supplementary Figure 3a), where Indomalaya had the lowest average climate connectivity and Oceania the highest. Median connectivity was comparable across realms for low elevation patches ($F = 0.393$, $p = 0.814$; Supplementary Figure 3a).

The proportion of total forest area that failed to connect to future analogous climate was higher when considering only high elevation patches. There were differences between biogeographic realms for both high and low elevation patches ($p < 0.001$; Supplementary Figure 3a), with the proportion of forest that was unsuccessful ranging from 36-63% for low elevation patches, and 68-84% for high elevation patches.

In summary, climate connectivity is poor even when restricting analyses to low elevation forests, which have greater potential to connect to cooler, higher elevation forest. The situation is worse for forest patches at high elevation, and species in these locations may have to rely upon alternative strategies to cope with climate change, such as local adaptation or translocation by humans.

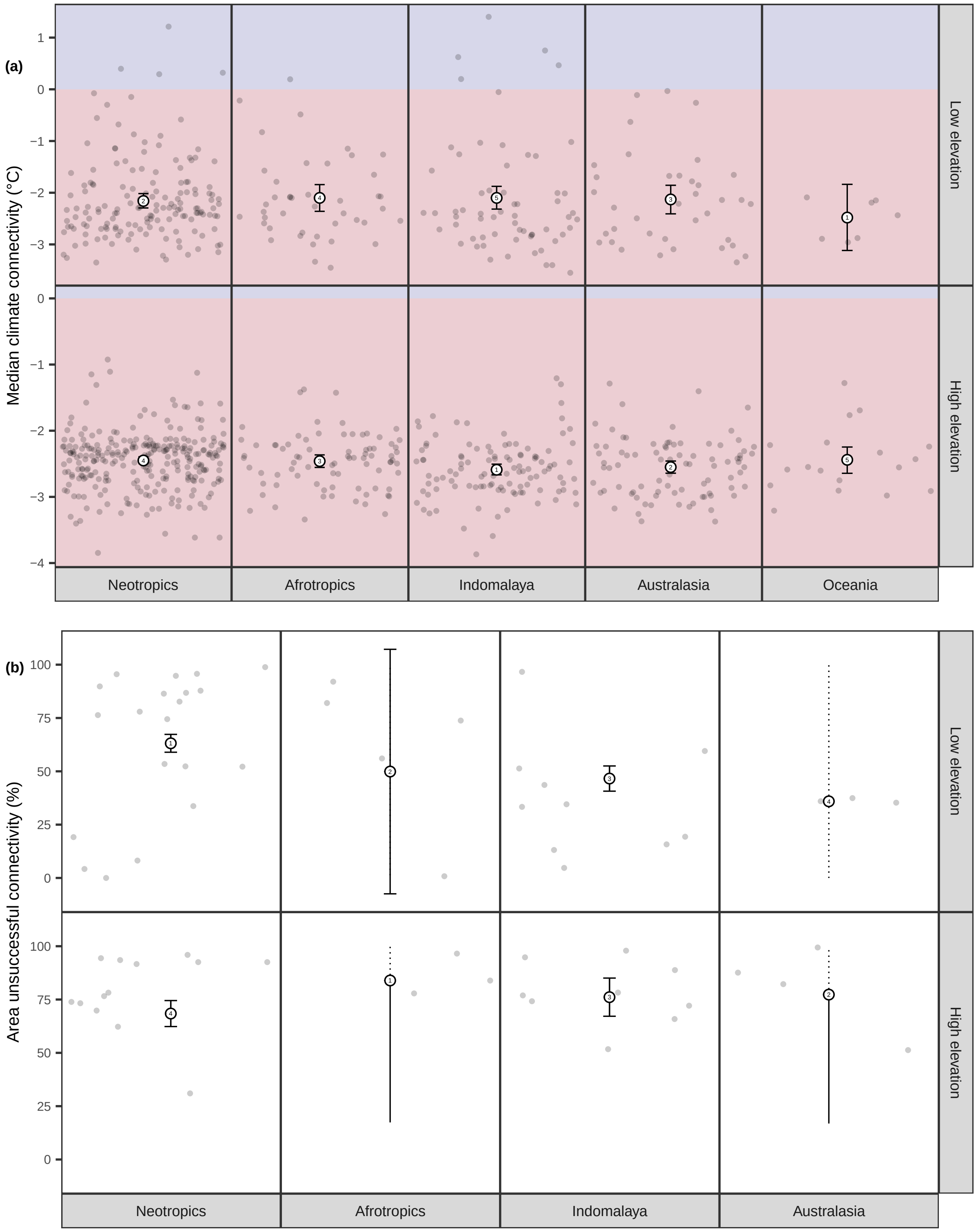

Supplementary Figure 3: Climate connectivity in the year 2012, for low and high elevation patches. Panel (a) shows results for median climate connectivity, with the dashed line indicating zero climate connectivity, at and above which successful climate connectivity is achieved. Panel (b) shows results for the proportion of total forested area that fails to achieve successful climate connectivity. Hollow circles are model-predicted values with 95% confidence intervals. The small number in the centre indicates rank: 1 corresponds to the smallest y value for that realm and dataset, through to 5 for the highest value. Raw data are plotted in the background as semi-transparent, filled points.

3 Supplementary Methods 3: Excluding tree plantations

3.1 Methods

The tree cover layers from Hansen et al. (2013) do not currently distinguish between natural forests and tree plantations. However, boundary polygons for tree plantations are available for seven countries: Brazil, Cambodia, Colombia, Indonesia, Liberia, Malaysia, and Peru (Transparent World, 2015). We therefore re-ran our analyses (see Methods in main text) for these seven countries only, with and without cells inside tree plantations. We buffered country polygons by 100 km to prevent artificial truncation of climate gradients (cf. McGuire et al., 2016). Statistical models were analogous to those in the main text (see Methods), except that biogeographic realm was not included as an explanatory variable because of the smaller and more uneven sample sizes in this subset of the data.

3.2 Results and Discussion

Median climate connectivity in 2012 was -1.17°C including cells in tree plantations, versus -1.2°C excluding tree plantations. Median climate connectivity did not differ by year in either case ($p > 0.05$; Figure 4a). Thus, regardless of the year or inclusion of tree plantations, typical tropical forest fails to connect patches to future analogous climates.

The percentage of forest that failed to achieve successful climate connectivity in 2012 was comparable regardless of whether tree plantations were included (37% if including plantations versus 40.4% excluding plantations), although the trends over time did differ. If cells inside plantations were included, there was a slight decrease (-2.9%) from 2000 to 2012 in the percentage of forest that was unsuccessfully connected ($F = 4.79$, $p < 0.05$; Figure 4b). The opposite was true when cells inside plantations were excluded ($F = 27.4$, $p < 0.001$; Figure 4b), with the proportion of unsuccessfully connected forest increasing by 8.7% from 2000 to 2012. The discrepancy between datasets in the effect of year is very likely driven by increasing tree cover inside tree plantations through the growth of planted trees.

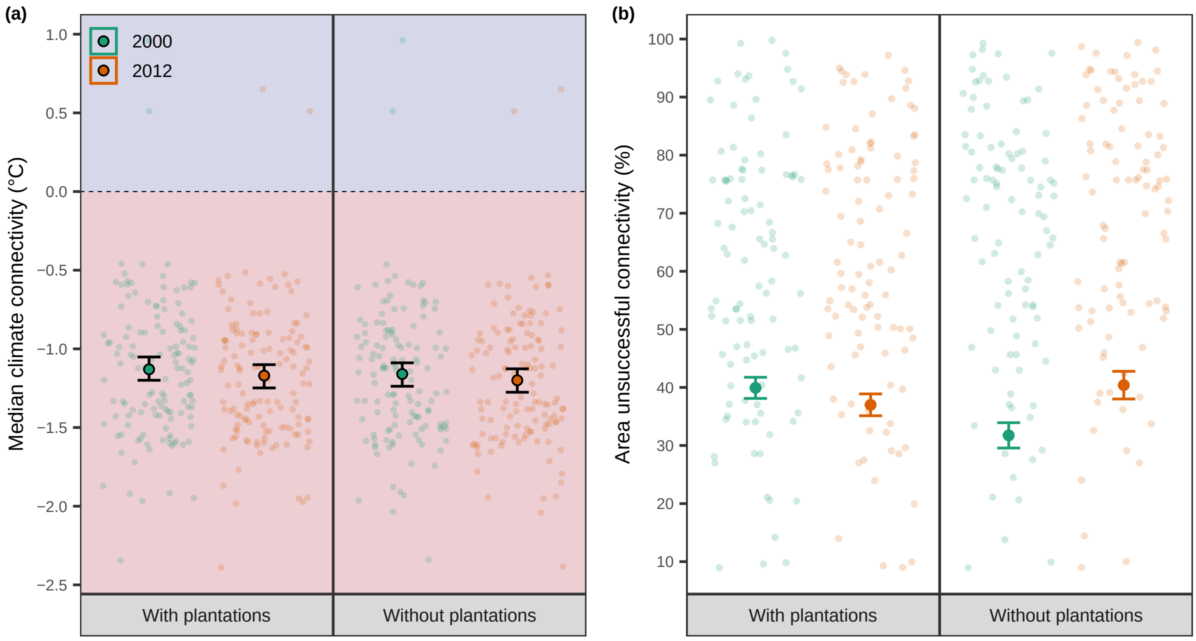

Supplementary Figure 4: Climate connectivity in the year 2000 (green) and 2012 (orange), including or excluding cells that fall inside tree plantations. Panel (a) shows results for median climate connectivity, with the dashed line indicating zero climate connectivity, at and above which successful climate connectivity is achieved. Panel (b) shows results for the proportion of total forested area that fails to achieve successful climate connectivity. Solid points are model-predicted values with 95% confidence intervals. Raw data are plotted in the background as semi-transparent points.

From 2000 to 2012, loss of climate connectivity increased with increasing loss of forest area. This was true whether including tree plantations ($F = 96.4$, $p < 0.001$; Figure 5) or excluding tree plantations ($F = 41.5$, $p < 0.001$; Figure 5). The relationship for both datasets was weaker than in the full model (see main text), and when including plantations the relationship appeared to invert for very high loss of forest area. These results may be caused by the smaller sample size and truncation of climate gradients (e.g. from the Amazon to parts of the Andes) when focusing only on countries with tree plantation data. It is also possible that very high loss of forest area is concentrated in places which have already lost climate connectivity, and therefore have little left to lose.

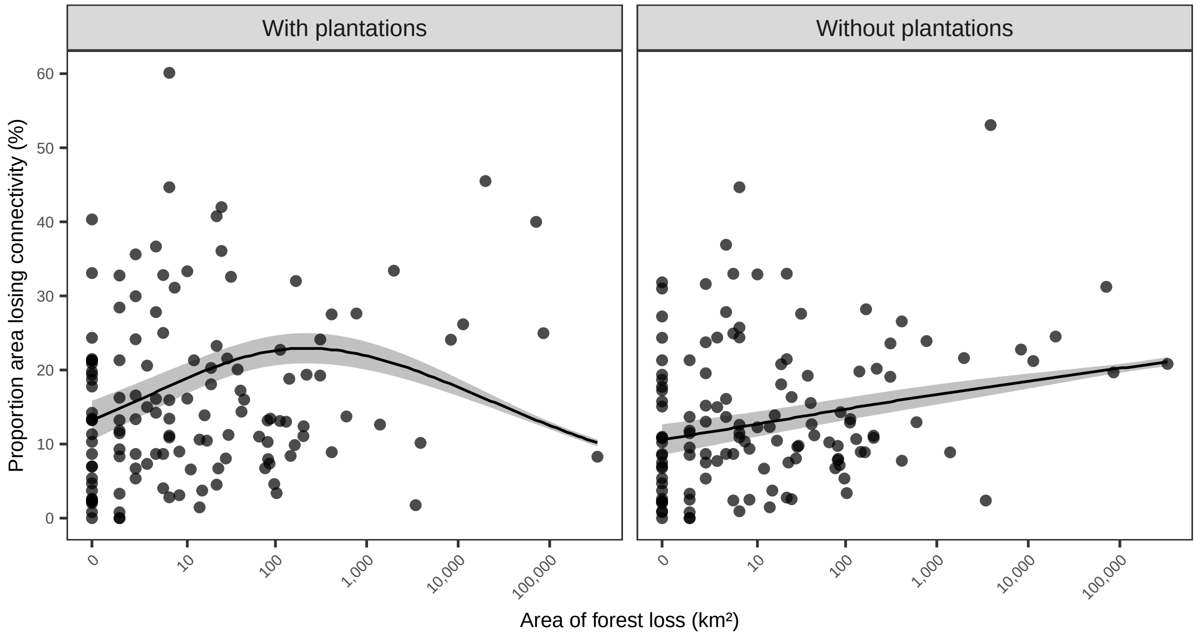

Supplementary Figure 5: The proportion of total forested area in each land mass that lost climate connectivity between 2000 and 2012 with increasing area of forest loss, including versus excluding cells inside tree plantations. Points correspond to raw data. Fitted lines derive from model predictions with 95% confidence intervals.

4 Supplementary Methods 4: Different RCP scenarios

4.1 Methods

In the main text we used Representative Concentration Pathway (RCP) 8.5 to derive Mean Annual Temperature in the year 2070. This is the most severe (‘business-as-usual’) IPCC scenario (IPCC, 2013), which has thus far been the best predictor of observed climate change (Sanford et al., 2014). However, it is possible that by 2070 stronger mitigating action is taken. We therefore repeated our analyses using RCP2.6, which is the least severe warming scenario. All methods were identical to those in the main text, changing only the layer used for future temperature.

4.2 Results and Discussion

For both RCP scenarios, median climate connectivity differed between realms ($p < 0.001$; Supplementary Figure 6a), being lowest in the Neotropics, Afrotropics and Indomalaya and highest in Australasia and Oceania. Median climate connectivity was below zero for both scenarios, but less negative for RCP2.6 than RCP8.5. The implication is that forest patches across the tropics will generally fail to facilitate species range shifts to the extent that species could completely avoid climate warming, but with mitigation the amount of warming experienced would be less.

The proportion of forest area that failed to achieve successful climate connectivity (≥ 0) in the year 2012 was influenced by biogeographic realm in both RCP scenarios ($p < 0.001$; Supplementary Figure 6b). All realms were less successfully connected using RCP8.5 (percentage area that was unsuccessful ranged from 37-70% in RCP8.5 vs. 16-36% in RCP2.6) and the ranking of different realms was also different depending on the RCP scenario. In both scenarios, Indomalaya and Oceania were among the least successfully connected and Australasia the best. Overall, these results suggest that despite the low average climate connectivity in both scenarios of future warming, strong mitigation like that assumed under RCP2.6 could maintain high climate connectivity in large forest patches.

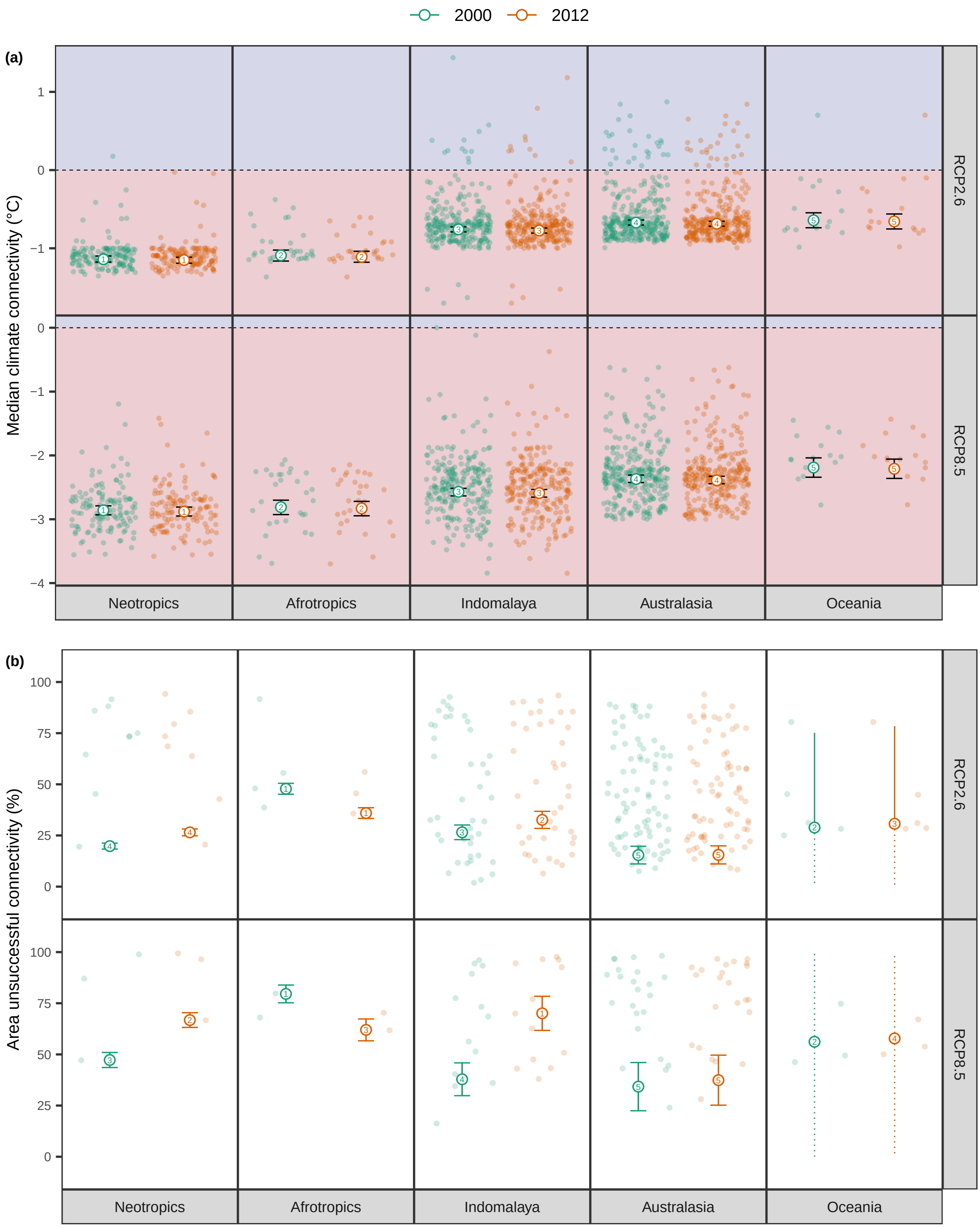

Supplementary Figure 6: Climate connectivity in the year 2000 (green) and 2012 (orange), for RCP2.6 (least severe warming scenario) and RCP8.5 (most severe warming scenario). Panel (a) shows results for median climate connectivity, with the dashed line indicating zero climate connectivity, at and above which successful climate connectivity is achieved. Panel (b) shows results for the proportion of total forested area that fails to achieve successful climate connectivity. Hollow circles are model-predicted values with 95% confidence intervals. The small number in the centre indicates rank: 1 corresponds to the smallest y value for that realm and dataset, through to 5 for the highest value. Raw data are plotted in the background as semi-transparent, filled points. Confidence intervals in panel (b) are plotted with dotted lines where they extend beyond 0 or 100%.

For both RCP scenarios we found that median climate connectivity did not change between 2000 and 2012 ($p > 0.05$), and this was consistent across biogeographic realms ($p > 0.05$; Supplementary Figure 6a). Similarly, while the proportion of forest area that failed to achieve successful climate connectivity was higher in 2012 than 2000 under RCP8.5 ($F = 13.6$, $p < 0.001$; Supplementary Figure 6b), there was no difference between years under RCP2.6 ($F = 1.64$, $p = 0.201$; Supplementary Figure 6b). Under both scenarios the effect of year depended on the biogeographic realm ($p < 0.001$), with the biggest losses in the Neotropics and Indomalaya compared to a decrease in the Afrotropics (Supplementary Figure 6b).

The proportion of forest experiencing a decrease in climate connectivity from 2000 to 2012 was influenced by both the area of forest loss ($p < 0.001$) and biogeographic realm ($p < 0.001$; Supplementary Figure 7), in both RCP scenarios. Indomalaya and the Neotropics experienced substantial loss of climate connectivity in both scenarios, while the magnitude of change varied between scenarios for the Afrotropics, Oceania and Australasia (Supplementary Figure 7). In both scenarios the relationship between connectivity loss and forest loss is non-linear, however under RCP2.6 the steepness of this relationship decreased for very high values of forest loss more-so than under RCP8.5. This discrepancy should be interpreted with caution since there are only a small number of datapoints at the upper end of the relationship, but the implication is that there is a greater propensity for climate connectivity loss to accelerate under a business-as-usual scenario compared to a strong mitigation scenario.

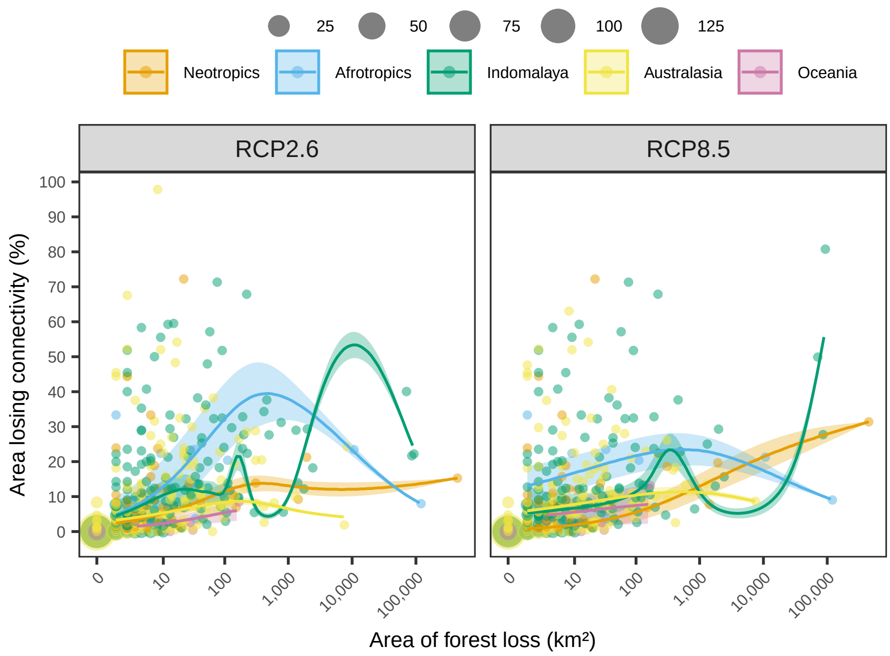

Supplementary Figure 7: The proportion of total forested area in each land mass that lost climate connectivity between 2000 and 2012, with increasing area of forest loss and across different biogeographic realms (orange = Neotropics, blue = Afrotropics, green = Indomalaya, yellow = Australasia and pink = Oceania). Points correspond to raw data, with point size indicating the number of observations at that value. Fitted lines derive from model predictions with 95% confidence intervals.

5 Supplementary Methods 5: Including roads and rivers as barriers

For some taxa and in some regions, linear features such as roads and rivers act as barriers to species movement (Oliveira et al., 2017; Shepard et al., 2008). We capture this to some extent in our study because such features appear as non-forest habitat, separating nearby forest patches and preventing them from being identified as neighbours. However, because we aggregate forest patches that are the same temperature and within 2 km of each other, some patches may contain linear features that in reality would act as hard barriers to movement.

To investigate the impact of linear features as barriers to range shifts we recalculated climate connectivity for mainland Central and South America, where major rivers of the Amazon are thought to limit species' distributions. We used the Global River Widths from Landsat (GRWL) Database (Allen and Pavelsky, 2018) to identify rivers with a minimum width of 1 km or more, and the Global Roads Inventory Project (GRIP) (Meijer et al., 2018) to identify highways. The method for calculating climate connectivity was the same as that used in the main text, except that patches were prevented from aggregating across major rivers or highways. Qualitatively, Supplementary Figure 8a suggests that the inclusion of barriers has little effect on the overall results, and may even improve climate connectivity (Supplementary Figure 8b). While counter-intuitive, barriers could increase overall climate connectivity if they force an alternative route, with a final destination patch that is ultimately cooler under climate warming than the original destination would have been.

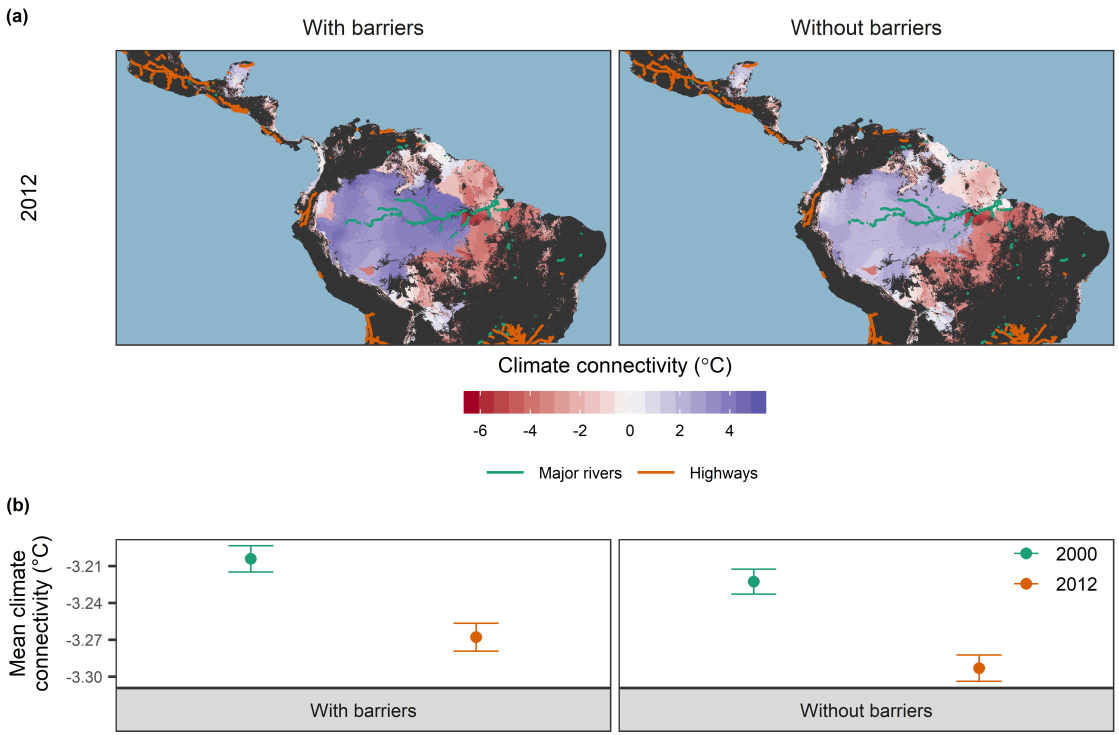

Supplementary Figure 8: Climate connectivity in 2012 for mainland Central and South America, with and without highways and major rivers as barriers. As in the main text (Figure 1), positive cell values (blue) in the maps (a) indicate successful climate connectivity and negative cell values (red) indicate unsuccessful climate connectivity. Green lines are major rivers and orange lines are highways. Panel (b) summarises mean climate connectivity across patches within this land mass (± SE), for the years 2000 (green) and 2012 (orange).

6 Supplementary Methods 6: Null scenarios of random forest loss

In the main analyses there was a non-linear relationship of climate connectivity loss with increasing forest loss, which varied by biogeographic realm. Accelerating climate connectivity loss with increasing forest loss is to some degree inevitable, as redundant links between patches are removed and eventually connections to cooler destinations are lost completely. A similar pattern is seen in models of tropical forest fragmentation, whereby forest loss beyond a given threshold causes a disproportionate increase in the number of forest fragments (Taubert et al., 2018).

To further explore patterns of climate connectivity loss between 2000 and 2012, we compared the observed results to scenarios of random deforestation. Owing to computational constraints we focus only on Indomalaya, where different land masses experienced the full range of 0-100% forest loss between 2000 and 2012.

For each land mass we randomly removed 10, 20, 30, 40, 50, 60, 70 and 80% of all cells that were classed as forest in the year 2000. We created 100 null scenarios of forest cover in the year 2012 by randomly selecting one scenario of deforestation (from 10-80%) for each unique land mass. Thus, each of the 100 scenarios of forest cover in 2012 had the same total number of land masses (267), differing only in the amount of forest loss randomly assigned to each land mass.

Climate connectivity loss always accelerated with increasing deforestation (Supplementary Figure 9), but the observed patterns of connectivity loss were much less extreme than under random deforestation. We therefore speculate that concentrating forest loss in particular areas, in line with a land-sparing approach, is more likely to conserve regional climate connectivity than a piecemeal, scattered pattern of deforestation. The location of forest loss relative to particularly vital patch connections will also be crucial to resulting changes in regional climate connectivity.

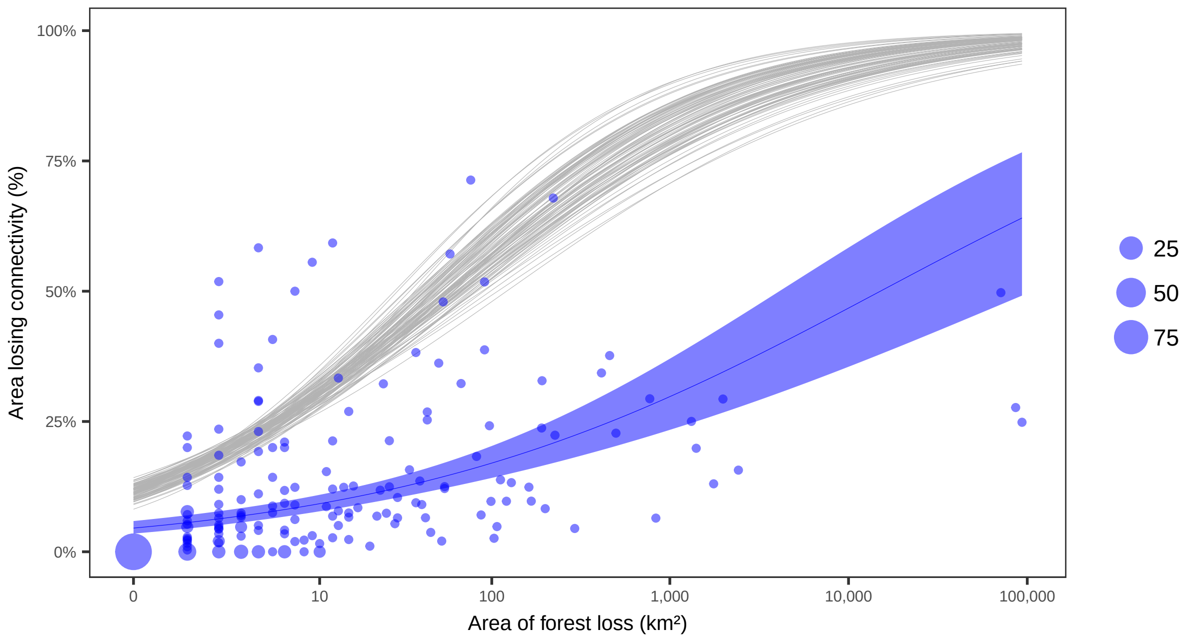

Supplementary Figure 9: Observed climate connectivity loss with increasing forest loss (blue), compared to climate connectivity loss with 100 scenarios of random forest loss (grey). Points correspond to raw data, with point size indicating the number of observations at that value. Fitted lines and confidence intervals were created using a quasi-binomial GLM (area losing climate connectivity versus area not losing climate connectivity) in the `geom_smooth` argument of `ggplot2::ggplot` in R (Wickham, 2016).

7 Supplementary Methods 7: Worked example

The following text provides a step-by-step calculation of climate connectivity in the Brazilian states of Rondônia and Mato Grosso.

7.1 Step 1: Creating forest patches

Climate connectivity is calculated using climate-partitioned patches of natural habitat (McGuire et al., 2016). In this study natural habitat refers to tropical forest, derived from Hansen et al. (2013) for the years 2000 and 2012. For the year 2000, cells were classed as forested if they had > 50% tree cover (Figure 10a; Hansen et al., 2013). For the year 2012, cells were classed as forest based on forest loss and forest gain, relative to forest cover in 2000 (Figure 10b). If a cell experienced forest loss, it had gone from a forested to non-forested state between 2000 and 2012 and was classed as non-forest. If a cell had experienced forest gain, it had gone from a non-forested to forested state between 2000 and 2012; providing there had been no concomitant loss, the cell was classed as forest. All subsequent steps were applied separately to forest cover in 2000 and 2012.

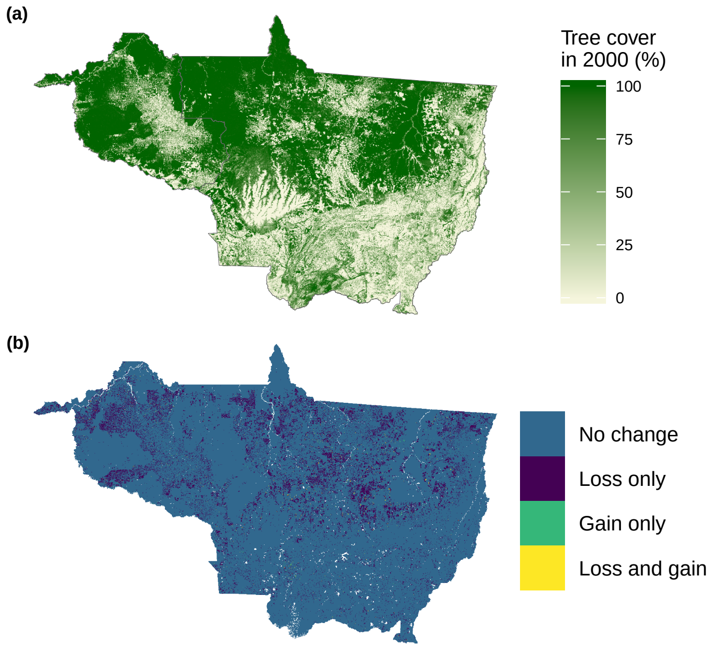

Supplementary Figure 10: Tree cover in the year 2000 (a) ranges from low (beige) to high (dark green). Tree cover change from 2000 to 2012 (b) includes: no change (blue), forest loss (purple), forest gain (green) or both loss and gain (yellow). Both layers derive from Hansen et al. (2013), and are used to classify cells into either forest or non-forest in the years 2000 and 2012.

We used Mean Annual Temperature (MAT) as our climate variable, which is the first bioclimatic variable of the WorldClim database (Version 1.4; Hijmans et al., 2005). All layers (forest cover and climate data) were projected into the World Cylindrical Equal Area projection and re-sampled to 1 km^2 resolution. Current climate (~1950-2000) was assigned to forested cells, and rounded to increments of 0.5°C. Adjacent cells with the same temperature were assigned to the same patch (Figure 11). Patches less than 10 km^2 in area were removed, and patches within 2 km of each other were assigned to the same patch. Once forest patches had been determined we also calculated their future temperature in the year 2070 (2061-2080), using data from the HadGEM2-AO general circulation model (IPCC, 2013) and Representative Concentration Pathway (RCP) 8.5, which is the most severe ('business-as-usual') IPCC scenario.

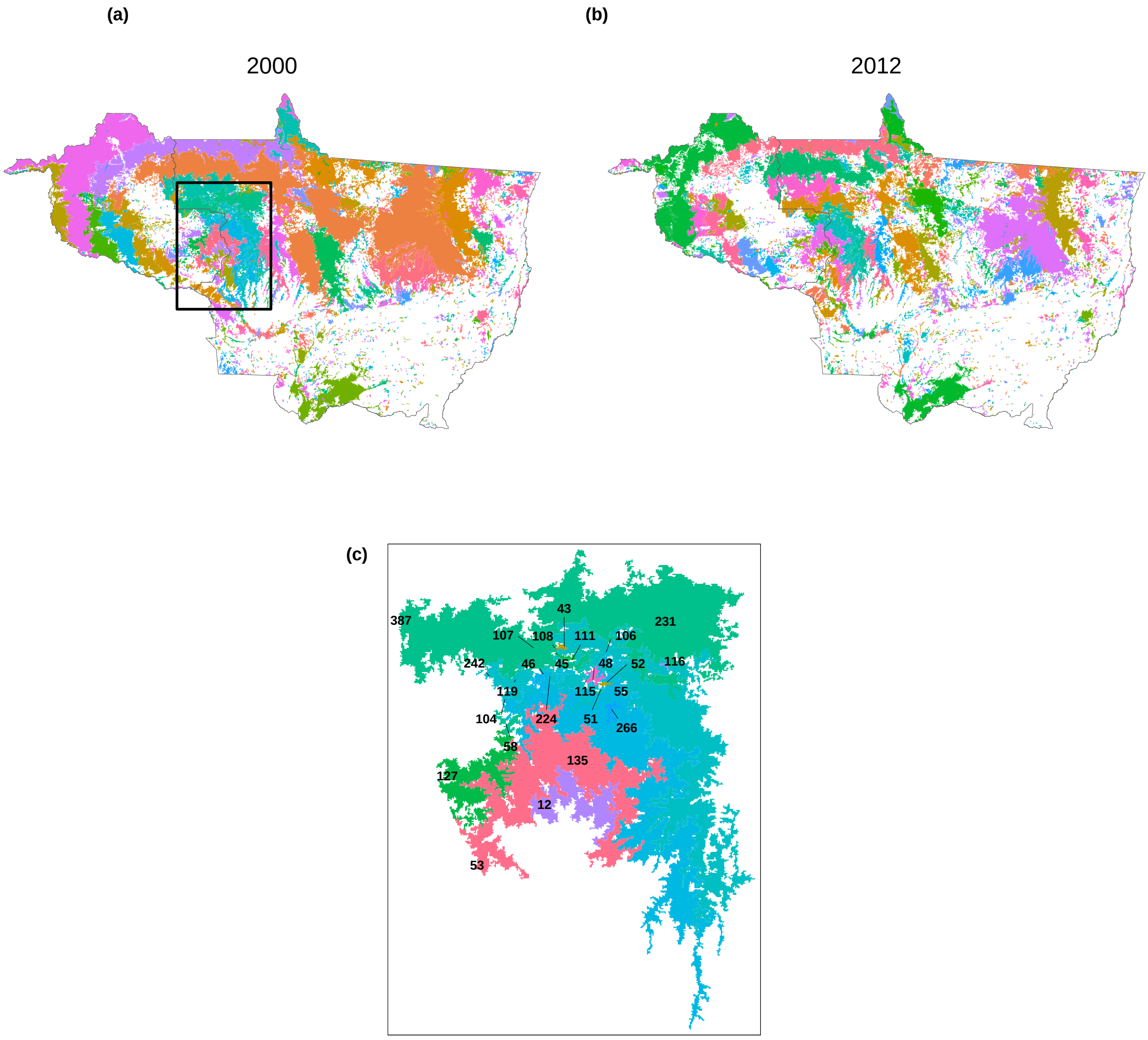

Supplementary Figure 11: Forest patches in 2000 (a) and 2012 (b). Black inset (c) corresponds to magnified view of the subset of patches used below to calculate climate connectivity. Shading indicates unique patches and numbers correspond to patch identities, a sample of which can be found in Table 1.

7.2 Step 2: Identifying destination patches

Climate connectivity for a given patch depends on the difference between the current temperature of that patch, and the future temperature of the coolest patch that can be reached by traversing a gradient of hotter to cooler adjacent patches (McGuire et al., 2016). The aim of this next step, therefore, was to determine the coolest destination patch for each origin patch.

We first identified, for each pair of neighbouring patches, which of the two was the hotter 'origin' patch and which was the cooler 'destination' patch. In the code snippets below, `nbr` refers to a dataframe of patch neighbours, and `temp_dat` is a dataframe of the current and future temperature for all patches.

(a)

patch1	patch2	temp1	temp2
12	53	22.0	22.5
43	108	22.7	22.9
43	224	22.7	23.5
43	387	22.7	24.0
45	111	22.6	22.9
45	224	22.6	23.5

(b)

origin	dest	origin_temp	dest_temp
53	12	22.5	22.0
108	43	22.9	22.7
224	43	23.5	22.7
387	43	24.0	22.7
111	45	22.9	22.6
224	45	23.5	22.6

Supplementary Table 1: Dataframe of patch neighbours before (a) and after (b) sorting neighbours into either the hotter origin patch or cooler destination patch.

Most patches have multiple neighbours, so we next identified *all* the neighbours for each origin patch (assigned to `connections`). For example, we can see below that origin patch 266 has only one neighbour: patch 104. Patch 231 has no neighbours, and patch 224 has many.

```
connections <-
    sapply(1:nrow(temp_dat), function(x){
        nbr$dest[nbr$origin == temp_dat[x,"patch"]]
    })
names(connections) <- temp_dat$patch
tail(connections)
```

```
## $`135`
## [1] 53
##
## $`224`
##  [1]  43  45  48  51  52  53 104 106 108 111 115 116
##
## $`231`
## integer(0)
##
## $`242`
```

```
## [1]  46 104 119
##
## $`266`
## [1] 104
##
## $`387`
## [1]  43 104 107 108 111 116 224 231 242
```

To determine the final, coolest destination patch that can be reached from each origin patch, we traced the path according to which of the immediate neighbours was the coolest. This step was done by iterating over unique patch temperatures (`uniquetemps`), from cooler to hotter.

```
uniquetemps <- sort(unique(temp_dat$temp))
uniquetemps
```

```
##  [1] 22.0 22.5 22.6 22.7 22.8 22.9 23.0 23.1 23.3 23.5 23.6 24.0
```

We created variables in `temp_dat` to populate with the temperature and patch identity of the final destination patch for each origin patch, and created a copy of this dataframe called `running`. The dataframe `running` is updated with each iteration.

```
# Set up output columns
temp_dat$dest <- NA
temp_dat$dest_temp <- NA
temp_dat$inter_patch <- NA


# Copy the original dataframe
running <- temp_dat[, c("patch", "temp")]
```

In each iteration through unique temperatures (from cooler to warmer) we identified:

- The origin patches that corresponded to that temperature
- The coolest neighbour of each origin patch

And subsequently we:

- Populated the empty columns in our original dataframe with the patch identity and temperature of the final destination patch of the coolest neighbour
- Updated the `running` dataframe, to track the pathway from each origin patch to its final destination patch (which may or may not be an immediate neighbour)

The iterations below were run in a loop, but for illustrative purposes we will iterate over each unique temperature manually.

7.2.1 Iteration 1

We begin by defining the focal unique temperature of this iteration. In this case, it's the first (i.e. coolest) value from our previously defined vector of unique temperatures, `uniquetemps`.

```
this_temp <- uniquetemps[1]
this_temp
```

```
## [1] 22
```

Next we define the indices of all patches that are 22°C (`inds`).

```
inds <- which(running[,"temp"] == this_temp)
running[inds, "patch"]
```

```
## [1] 12
```

Patch number 12 is the only patch at this temperature. Now we need to see if patch 12 has any associated destination patches:

```
length(connections[[inds]]) > 0
```

```
## [1] FALSE
```

No, therefore the final destination patch and the final destination temperature are the same as the origin: patch 12, temperature 22°C. The reason that we use the `running` dataframe (a copy of the original `temp_dat` dataframe) to retrieve the temperature and identity of the destination patch will become clear in later iterations (i.e. Iteration 5).

```
temp_dat$dest[inds]<- running[inds, "patch"]
temp_dat$dest_temp[inds]<- this_temp
```

Let's look at the row in our dataframe that we have just populated:

```
temp_dat[inds,]
```

```
##   patch temp ftemp dest dest_temp inter_patch
## 1    12   22    25   12        22          NA
```

Note that because the origin and destination patch are the same, there are no intermediate patches and so the value for `inter_patch` remains NA.

7.2.2 Iteration 2

Moving onto the next unique temperature. This iteration is more complicated because the origin patch *does* have one or more neighbouring destination patches.

```
this_temp <- uniquetemps[2]
this_temp
```

```
## [1] 22.5
```

Again we define the indices of all patches that have this temperature (22.5°C).

```
inds <- which(running[,"temp"] == this_temp)
running[inds, "patch"]
```

```
## [1] 53 58
```

This time both patch 53 and patch 58 have the temperature that we're interested in. We start with patch 53 (index 1 in the vector `inds`).

Are there any associated destination patches?

```
length(connections[[inds[1]]]) > 0
```

```
## [1] TRUE
```

Yes. We define the indices of the destination patches as well (dest_inds).

```
dest_inds <- which(temp_dat$patch %in%  connections[[inds[1]]])
```

There may be multiple destination patches, so we need to identify the minimum temperature across all of them (t), as well as the index of the patch (or patches) that correspond to this minimum temperature (min_ind).

```
t <- min(running[dest_inds, "temp"])
t
```

```
## [1] 22
```

```
min_ind <- which(running[dest_inds, "temp"] == t)
```

Is there more than one destination patch that has this minimum temperature (22°C)?

```
length(min_ind) > 1
```

```
## [1] FALSE
```

No, so min_ind is the index of the destination patch that we're interested in. If there were more than one destination patch with the same minimum temperature, the first would be used arbitrarily.

Which patch does this index correspond to?

```
temp_dat$patch[min_ind]
```

```
## [1] 12
```

Patch 12. This is the final destination patch for patch 53. We assign the final temperature (22°C) and the identity of the final destination patch (12) to the associated origin patch (53) in our original dataframe, temp_dat.

```
temp_dat$dest_temp[inds[1]] <- t
temp_dat$dest[inds[1]] <- running$patch[min_ind]
```

We must also update the running dataframe so that patch 53 acquires the temperature and identity of patch 12. This step is vital for constructing more complicated pathways. In this example, since the final destination of patch 53 is patch 12, any origin patches in subsequent iterations whose neighbouring destination is patch 53 (see Iteration 5) will be assigned the final destination temperature and identity of patch 12, *not* patch 53.

```
running$temp[inds[1]] <- t
running$patch[inds[1]] <- running$patch[min_ind]
```

Finally, we capture intermediate patches that are traversed from origin to destination. The path from patch 53 to patch 12 cannot have intermediate patches because patch 12 is its own destination (there were no neighbouring patches that were cooler; see Iteration 1).

```
inter_patch <- temp_dat[min_ind, "inter_patch"]
is.na(inter_patch)
```

```
## [1] TRUE
```

We assign the final destination patch as the only intermediate patch. This is not strictly necessary since we have already recorded patch 12 as part of the path because it is the destination. However, this step highlights the fact that in this iteration the destination patch is not the same as the origin patch.

```
temp_dat$inter_patch[inds[1]] <- temp_dat[min_ind, "patch"]
```

We can now check the row for patch 53 in `temp_dat` and in the `running` dataframe. Note how in the `running` dataframe the row associated with patch 53 now has the identity and temperature of patch 12 instead.

```
temp_dat[inds[1],]
```

```
##   patch temp ftemp dest dest_temp inter_patch
## 8    53 22.5  25.6   12        22          12
```

```
running[inds[1],]
```

```
##   patch temp
## 8    12   22
```

Remembering that there were two origin patches corresponding to the focal temperature of this iteration (22.5°C), we must now repeat the above process for patch 58 (index 2 in the vector `inds`).

Does patch 58 have any neighbouring destination patches?

```
length(connections[[inds[2]]]) > 0
```

```
## [1] FALSE
```

No. As with Iteration 1, we assign the final destination temperature and patch identity to be the same as the origin.

```
temp_dat$dest[inds[2]]<- running[inds[2], "patch"]
temp_dat$dest_temp[inds[2]]<- this_temp
temp_dat[inds[2],]
```

```
##    patch temp ftemp dest dest_temp inter_patch
## 10    58 22.5  25.5   58      22.5          NA
```

7.2.3 Iteration 5

We will now skip ahead to the fifth unique temperature, which illustrates the importance of updating the `running` dataframe in each iteration and using this to assign the temperature and identity of the final destination patch.

```
this_temp <- uniquetemps[5]
this_temp
```

```
## [1] 22.8
```

```
inds <- which(running[,"temp"] == this_temp)
running[inds, "patch"]
```

```
## [1] 135
```

Patch 135 is the only origin patch that is 22.8°C. Does it have any neighbouring destination patches?

```
length(connections[[inds[1]]]) > 0
```

```
## [1] TRUE
```

```
dest_inds <- which(temp_dat$patch %in%  connections[[inds[1]]])
```

Yes. Of the one or more neighbouring destination patches, what is the minimum temperature and what is the index of the corresponding patch?

```
t <- min(running[dest_inds, "temp"])
t
```

```
## [1] 22
```

```
min_ind <- dest_inds[which(running[dest_inds, "temp"] == t)]
```

Is there more than one destination patch at this minimum temperature (22°C)?

```
length(min_ind) > 1
```

```
## [1] FALSE
```

```
temp_dat$patch[min_ind]
```

```
## [1] 53
```

No. Patch 53 is the destination for patch 135. At this point, note that patch 53 was encountered in Iteration 2, and is itself connected to patch 12. As such, the row corresponding to the index of patch 53 actually has the temperature and identity of patch 12:

```
running[min_ind,]
```

```
##   patch temp
## 8    12   22
```

Because the final destination temperature and patch identity are retrieved from the `running` dataframe, we assign the final destination identity and temperature as patch 12, 22°C.

```
temp_dat$dest_temp[inds[1]] <- t
temp_dat$dest[inds[1]] <- running$patch[min_ind]
```

We again update the `running` dataframe. In subsequent iterations any origin patch whose coolest neighbour is patch 135 will also be assigned the final destination temperature and identity of patch 12.

```
running$temp[inds[1]] <- t
running$patch[inds[1]] <- running$patch[min_ind]
```

Lastly, we define the intermediate patches.

```
inter_patch <- temp_dat[min_ind, "inter_patch"]
is.na(inter_patch)
```

```
## [1] FALSE
```

In this case, of course, there *is* an intermediate patch between the origin and the destination – patch 53. We paste this patch together with the final destination to construct the full pathway from origin to destination.

```
temp_dat$inter_patch[inds[1]] <-
    paste(temp_dat[min_ind, "patch"],
          inter_patch[!(is.na(inter_patch))],
          sep = ";")
```

Let's inspect the rows that we have just populated:

```
temp_dat[inds[1],]
```

```
##    patch temp ftemp dest dest_temp inter_patch
## 20   135 22.8  25.9   12        22       53;12
```

```
running[inds[1],]
```

```
##    patch temp
```

```
## 20      12    22
```

7.3 Step 3: Calculating climate connectivity

At this point we know the current and future temperature of all patches (Step 1), and the identity and current temperature of their final destination patches (Step 2). Combining this information we can easily assign to each origin patch the future temperature of its destination patch:

```
temp_dat$dest_ftemp <-
    vapply(1:nrow(temp_dat), function(x){
        dest <- temp_dat$dest[x]
        dest_ftemp <- temp_dat$ftemp[temp_dat$patch == dest]
        return(dest_ftemp)
    }, FUN.VALUE = numeric(1))
```

Finally, we calculate climate connectivity. Conceptually, climate connectivity is the maximum temperature difference that can be achieved by traversing a gradient of hotter to cooler adjacent patches. Mathematically, this is therefore calculated as the current temperature of the origin patch minus the future temperature of the destination patch. If this value is zero or positive then climate connectivity is successful – organisms could potentially reach a forest patch that, under climate change, is the same as or cooler than their current source patch.

```
temp_dat$clim_conn <- temp_dat$temp - temp_dat$dest_ftemp
```

Final results can be seen in Figure 12 and Table 2. Table 3 demonstrates what the `running` dataframe looks like after having updated for each iteration.

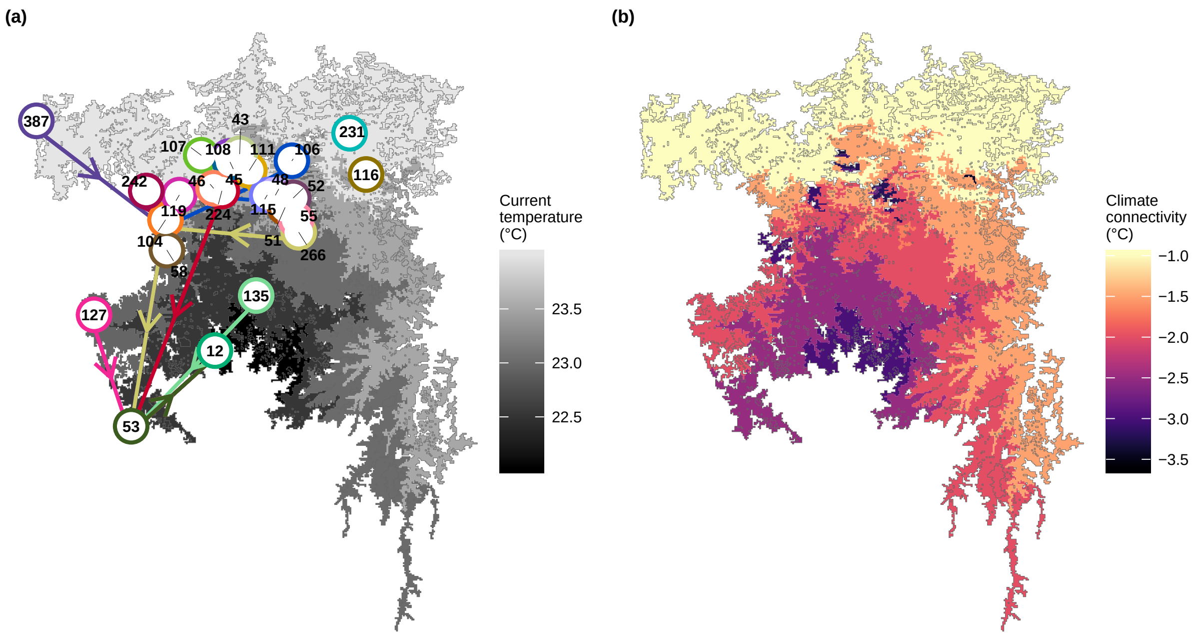

Supplementary Figure 12: Pathways from origin to destination patches (a) and climate connectivity across all patches (b). In panel a, patch shading corresponds to current mean annual temperature (°C), from cooler (black) to hotter (light grey). Circles indicate patch centroids; the numbers inside correspond to the patch identity (as in Tables 1, 2 and 3) and the arrows between indicate the direction of travel from hotter to cooler patches. In panel b, patch shading corresponds to climate connectivity (°C), measured as the current temperature of the origin patch minus the future temperature of the destination patch. If this value is zero or positive (not shown) the patch has achieved successful climate connectivity, meaning that species could reach analogous climate under future climate warming, given existing forest cover.

patch	temp	ftemp	dest	dest_temp	inter_patch	dest_ftemp	clim_conn
12	22.0	25.0	12	22.0	NA	25.0	-3.0
43	22.7	26.0	43	22.7	NA	26.0	-3.3
45	22.6	25.8	45	22.6	NA	25.8	-3.2
46	22.6	25.7	46	22.6	NA	25.7	-3.1
48	22.6	25.8	48	22.6	NA	25.8	-3.2
51	22.7	25.8	51	22.7	NA	25.8	-3.1
52	22.6	25.8	52	22.6	NA	25.8	-3.2
53	22.5	25.6	12	22.0	12	25.0	-2.5
55	22.6	25.8	55	22.6	NA	25.8	-3.2
58	22.5	25.5	58	22.5	NA	25.5	-3.0
104	23.0	26.1	12	22.0	53;12	25.0	-2.0
106	23.1	26.2	12	22.0	104;53;12	25.0	-1.9
107	22.9	26.5	107	22.9	NA	26.5	-3.6
108	22.9	26.1	43	22.7	43	26.0	-3.1
111	22.9	26.0	45	22.6	45	25.8	-2.9
115	23.0	26.1	48	22.6	48	25.8	-2.8
116	23.1	26.5	116	23.1	NA	26.5	-3.4
119	23.0	26.1	119	23.0	NA	26.1	-3.1
127	23.0	25.9	12	22.0	53;12	25.0	-2.0
135	22.8	25.9	12	22.0	53;12	25.0	-2.2
224	23.5	26.6	12	22.0	53;12	25.0	-1.5
231	23.6	26.9	231	23.6	NA	26.9	-3.3
242	23.5	26.5	12	22.0	104;53;12	25.0	-1.5
266	23.3	26.4	12	22.0	104;53;12	25.0	-1.7
387	24.0	27.1	12	22.0	104;53;12	25.0	-1.0

Supplementary Table 2: The results dataframe with final destination patches, final temperatures and climate connectivity for each origin patch.

patch	temp
12	22.0
43	22.7
45	22.6
46	22.6
48	22.6
51	22.7
52	22.6
12	22.0
55	22.6
58	22.5
12	22.0
12	22.0
107	22.9
43	22.7
45	22.6
48	22.6
116	23.1
119	23.0
12	22.0
12	22.0
12	22.0
231	23.6
12	22.0
12	22.0
12	22.0

Supplementary Table 3: The `running` dataframe, after updating with each iteration through unique temperatures. Note the repeated appearance of patch 12, which is a common final destination patch.

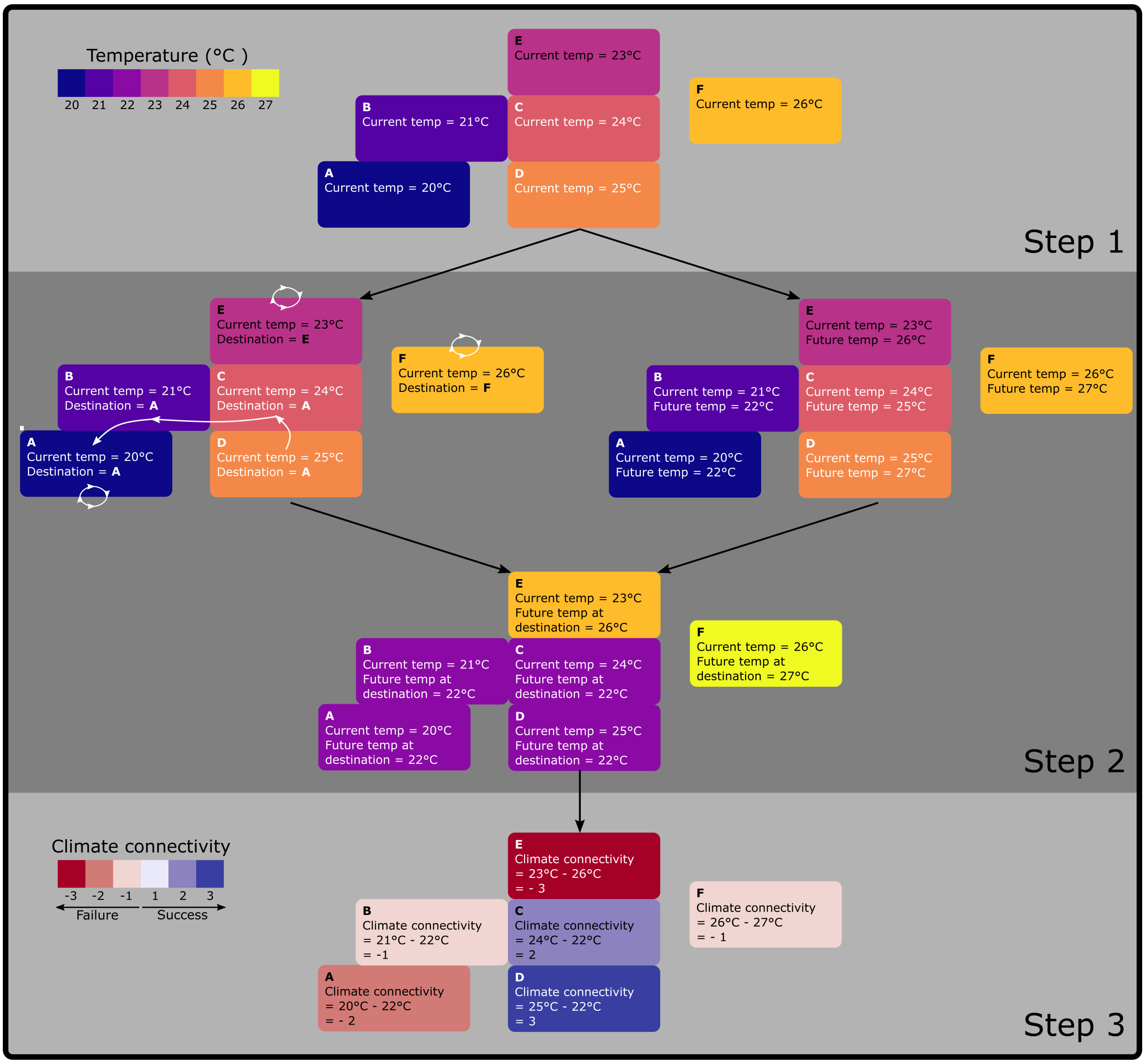

Supplementary Figure 13: Schematic diagram of the different steps involved in calculating climate connectivity.

8 Supplementary Figures

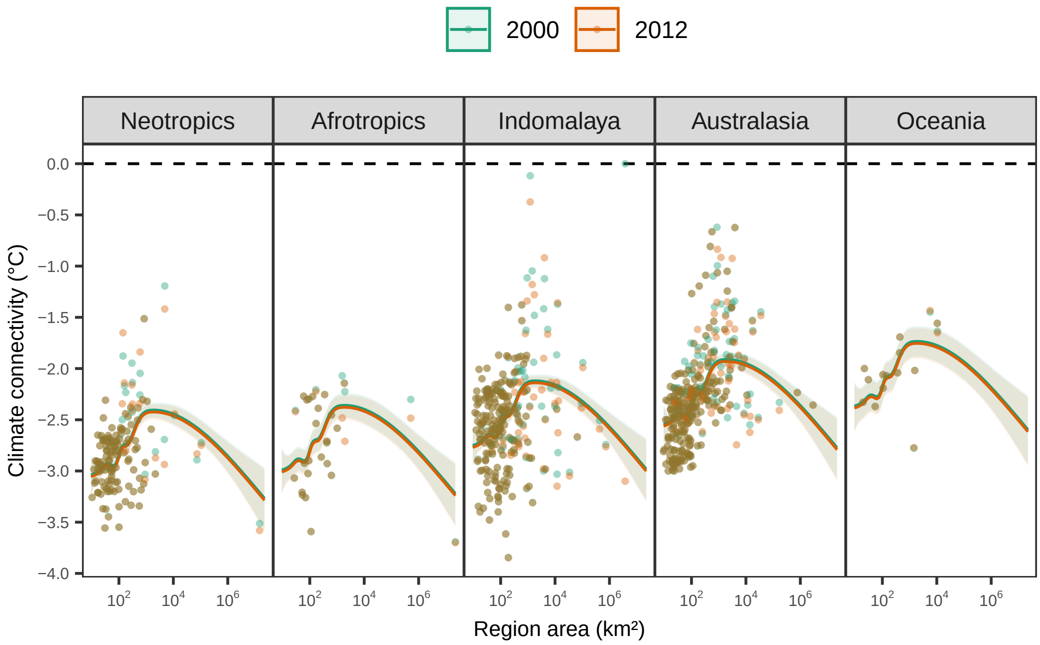

Supplementary Figure 14: Relationship between median climate connectivity and (log) land mass area, for the year 2000 (green) and 2012 (orange). Points correspond to raw data. Fitted lines derive from model predictions with 95% confidence intervals.

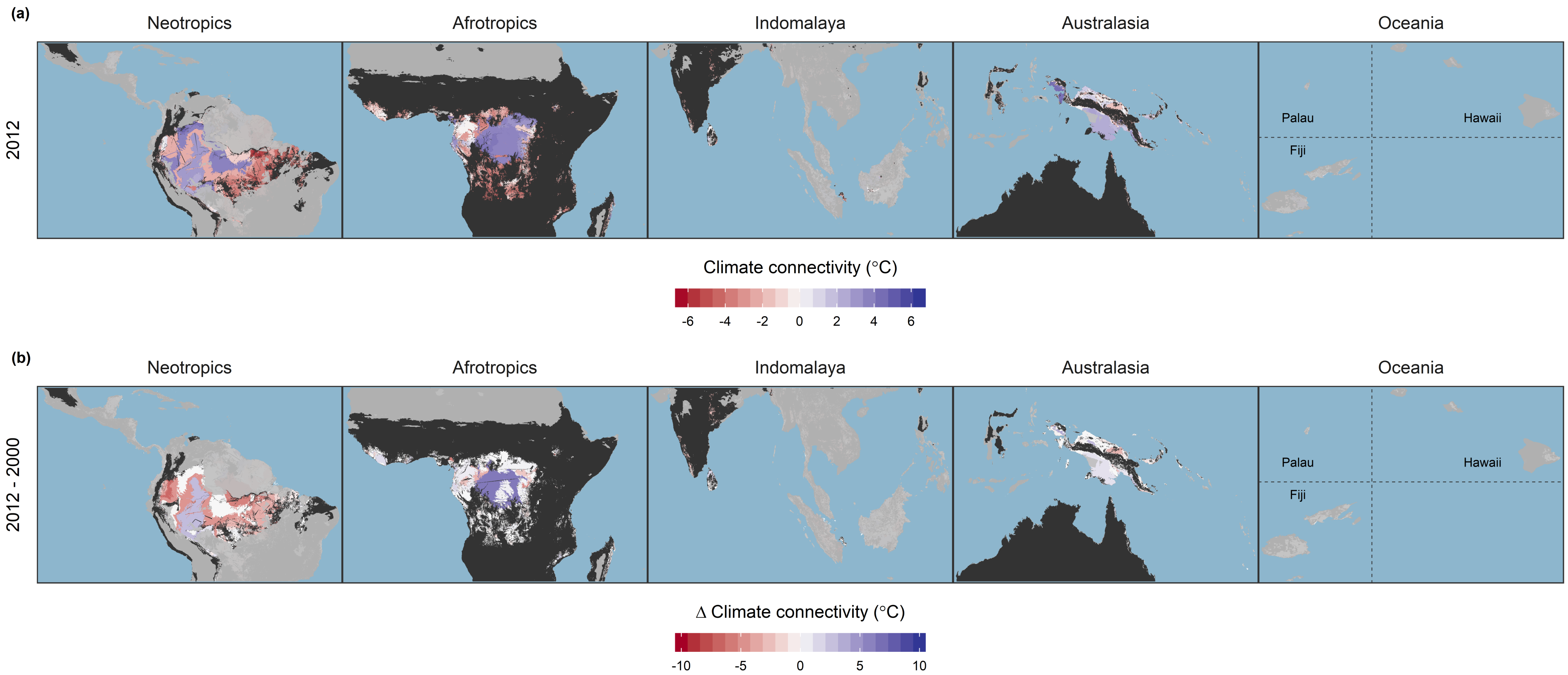

Supplementary Figure 15: Climate connectivity in 2012 (a) and change in climate connectivity from 2000 to 2012 (b) overlaid with areas of high climate vulnerability for mammals derived from Pacifici et al. (2018) (regions outside of these areas are masked in grey). We defined high vulnerability areas as those where more than 50% of mammal species had a negative predicted response to climate change. As in the main text (Figure 1), positive values (blue) indicate successful climate connectivity in panel (a), or a gain of connectivity in panel (b). Negative values (red) indicate unsuccessful climate connectivity in panel (a), or a loss of connectivity in panel (b). To aid visualisation we have shifted and magnified land masses in Oceania.

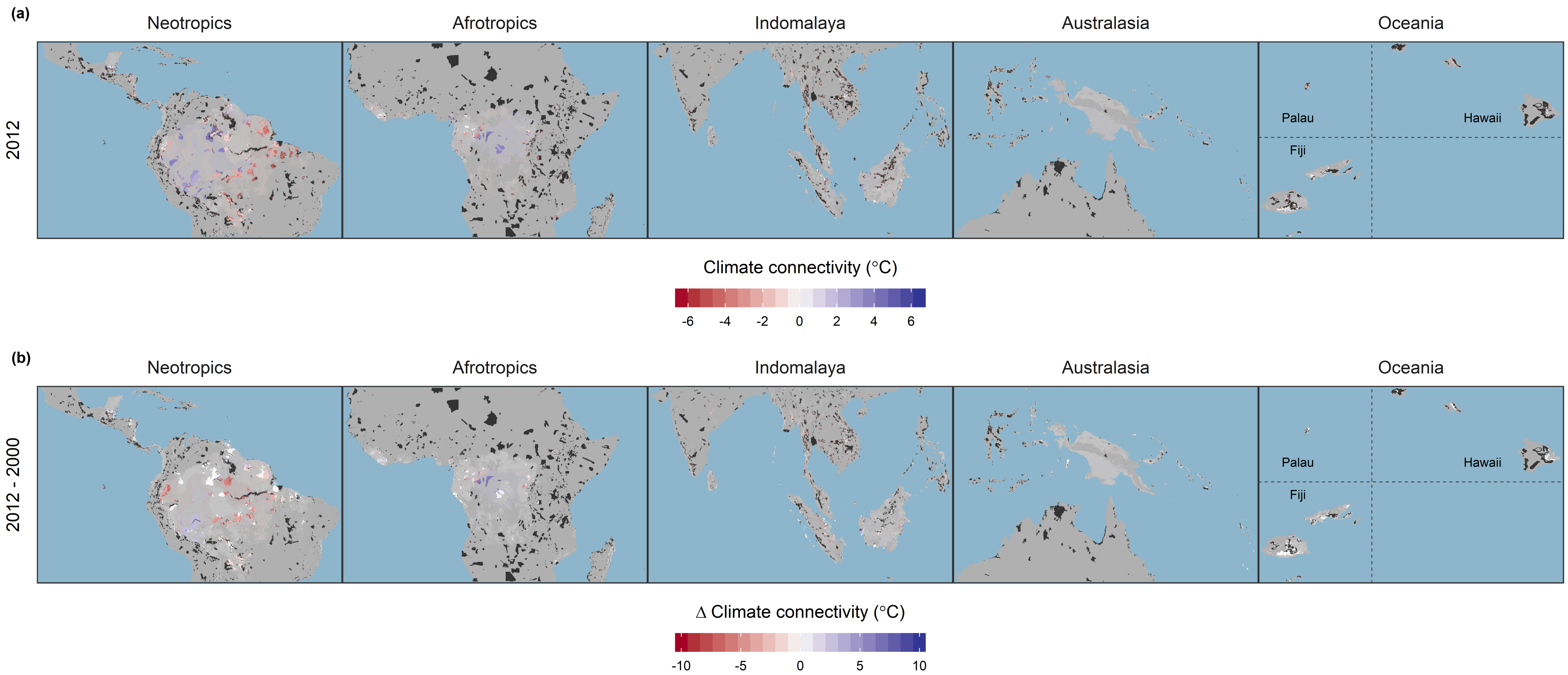

Supplementary Figure 16: Climate connectivity in 2012 (a) and change in climate connectivity from 2000 to 2012 (b) overlaid with Key Biodiversity Areas from BirdLife International (regions outside of these areas are masked in grey). As in the main text (Figure 1), positive values (blue) indicate successful climate connectivity in panel (a), or a gain of connectivity in panel (b). Negative values (red) indicate unsuccessful climate connectivity in panel (a), or a loss of connectivity in panel (b). To aid visualisation we have shifted and magnified land masses in Oceania.

9 Supplementary Tables

Supplementary Table 4: Summary of forest cover and forest cover change across the biogeographic realms of the tropics (rounded to three significant figures).

Realm	Forest area in 2000 (km^2)	Forest area in 2012 (km^2)	Forest loss (%)	Forest loss (km^2)	Forest gain (%)	Forest gain (km^2)
Neotropics	8,730,000	8,330,000	5.17	452,000	0.571	49,900
Afrotropics	3,910,000	3,790,000	3.36	131,000	0.352	13,700
Indomalaya	2,590,000	2,380,000	10.20	264,000	2.000	51,700
Australasia	968,000	955,000	1.48	14,300	0.197	1,910
Oceania	18,500	18,400	1.37	254	0.610	113
Total	16,200,000	15,500,000	21.60	862,000	3.730	117,000

Supplementary Table 5: Summary of model-predicted median climate connectivity across the biogeographic realms of the tropics. Values are for the years 2000 and 2012 under two scenarios of warming: RCP2.6 (strong mitigation scenario) and RCP8.5 (business-as-usual scenario), with upper and lower confidence intervals (CI).

RCP	Realm	Year	Median climate connectivity (°C)	Upper CI (°C)	Lower CI (°C)
RCP2.6	Neotropics	2000	-1.10	-1.10	-1.20
		2012	-1.20	-1.10	-1.20
	Afrotropics	2000	-1.10	-1.00	-1.20
		2012	-1.10	-1.00	-1.20
	Indomalaya	2000	-0.76	-0.73	-0.79
		2012	-0.77	-0.74	-0.81
	Australasia	2000	-0.67	-0.64	-0.70
		2012	-0.69	-0.65	-0.72
	Oceania	2000	-0.64	-0.55	-0.74
		2012	-0.66	-0.56	-0.75
RCP8.5	Neotropics	2000	-2.9	-2.8	-2.9
		2012	-2.9	-2.8	-2.9
	Afrotropics	2000	-2.8	-2.7	-2.9
		2012	-2.8	-2.7	-2.9
	Indomalaya	2000	-2.6	-2.5	-2.6
		2012	-2.6	-2.5	-2.7
	Australasia	2000	-2.4	-2.3	-2.4
		2012	-2.4	-2.3	-2.4
	Oceania	2000	-2.2	-2.0	-2.3
		2012	-2.2	-2.1	-2.4

Supplementary Table 6: Summary of model-predicted values for the proportion of forest area that fails to achieve successful climate connectivity (≥ 0), across the biogeographic realms of the tropics. Values are for the years 2000 and 2012 under two scenarios of warming: RCP2.6 (strong mitigation scenario) and RCP8.5 (business-as-usual scenario), with upper and lower confidence intervals (CI).

RCP	**Realm**	**Year**	**Area unsuccessful connectivity (%)**	**Upper CI (%)**	**Lower CI (%)**
RCP2.6	Neotropics	2000	20	21	18
		2012	27	28	25
	Afrotropics	2000	48	50	45
		2012	36	39	33
	Indomalaya	2000	27	30	23
		2012	33	37	28
	Australasia	2000	15	20	11
		2012	16	20	11
	Oceania	2000	29	75	NA
		2012	31	78	NA
RCP8.5	Neotropics	2000	47	51	44
		2012	67	70	63
	Afrotropics	2000	80	84	75
		2012	62	67	57
	Indomalaya	2000	38	46	30
		2012	70	78	62
	Australasia	2000	34	46	22
		2012	37	50	25
	Oceania	2000	56	NA	NA
		2012	58	NA	NA

Supplementary References

Allen, G.H., Pavelsky, T.M., 2018. Global extent of rivers and streams. Science 361, 585–588. doi:10.1126/science.aat0636

Hansen, M.C., Potapov, P.V., Moore, R., Hancher, M., Turubanova, S.A., Tyukavina, A., Thau, D., Stehman, S.V., Goetz, S.J., Loveland, T.R., Kommareddy, A., Egorov, A., Chini, L., Justice, C.O., Townshend, J.R.G., 2013. High-resolution global maps of 21st-century forest cover change. Science 342, 850–853. doi:10.1126/science.1244693

Hijmans, R.J., Cameron, S.E., Parra, J.L., Jones, P.G., Jarvis, A., 2005. Very high resolution interpolated climate surfaces for global land areas. International Journal of Climatology 25, 1965–1978. doi:10.1002/joc.1276

IPCC, 2013. Climate Change 2013: The Physical Science Basis. Contribution of Working Group I to the Fifth Assessment Report of the Intergovernmental Panel on Climate Change. Cambridge University Press, Cambridge, United Kingdom; New York, NY, USA.

McGuire, J.L., Lawler, J.J., McRae, B.H., Theobald, D.M., 2016. Achieving climate connectivity in a fragmented landscape. Proceedings of the National Academy of Sciences 113, 7195–7200. doi:10.1073/pnas.1602817113

Meijer, J.R., Huijbregts, M.A.J., Schotten, K.C.G.J., Schipper, A.M., 2018. Global patterns of current and future road infrastructure. Environmental Research Letters 13, 064006. doi:10.1088/1748-9326/aabd42

Oliveira, U., Vasconcelos, M.F., Santos, A.J., 2017. Biogeography of Amazon birds: Rivers limit species composition, but not areas of endemism. Scientific Reports 7, 2992. doi:10.1038/s41598-017-03098-w

Pacifici, M., Visconti, P., Rondinini, C., 2018. A framework for the identification of hotspots of climate change risk for mammals. Global Change Biology 24, 1626–1636. doi:10.1111/gcb.13942

Sanford, T., Frumhoff, P.C., Luers, A., Gulledge, J., 2014. The climate policy narrative for a dangerously warming world. Nature Climate Change 4, 164–166. doi:10.1038/nclimate2148

Shepard, D.B., Kuhns, A.R., Dreslik, M.J., Phillips, C.A., 2008. Roads as barriers to animal movement in fragmented landscapes. Animal Conservation 11, 288–296. doi:10.1111/j.1469-1795.2008.00183.x

Taubert, F., Fischer, R., Groeneveld, J., Lehmann, S., Müller, M.S., Rödig, E., Wiegand, T., Huth, A., 2018. Global patterns of tropical forest fragmentation. Nature. doi:10.1038/nature25508

Transparent World, 2015. Tree plantations. Available at: www.globalforestwatch.org.

Wickham, H., 2016. ggplot2: Elegant graphics for data analysis. Springer-Verlag New York.